Computational Sciences and Engineering 3(1) (2023) 55-75

University of Guilan

Computational Sciences and Engineering

journal homepage: https://cse.guilan.ac.ir/

FEM Analysis of the Effect of Using Environmentally Friendly Synthetic Materials on Reducing Pore Pressure in the Core of Rubble Mound Breakwaters

Nima Khorsandi [a], Payam Zanganeh Ranjbar [b,*], Seyed Ahmad Neshaei [b]

[a] Department of Civil Engineering, Ahrar University, Rasht, Guilan, Iran.
[b] Department of Civil Engineering, Faculty of Engineering, University of Guilan, Rasht, Iran.

ARTICLE INFO

Article history:
Received 7 April 2023
Received in revised form 4 june 2023
Accepted 3 July 2023
Available online 3 July 2023

Keywords:
Rubble mound breakwater
Pore pressure
Geotextile
Geodrain
Caspian sea

ABSTRACT

As a result of the waves crashing into the breakwater, a current will be created inside the breakwater, making the pore pressure. In this study, with the aim of pore pressure reduction, the replacement of environmentally friendly geosynthetic materials as part of the filter layer in the Rubble mound breakwaters (RMB) construction at the coastal area of the Caspian Sea was investigated through the finite element method (FEM) analysis. The results show that using the geodrain and geotextile to replace the filter materials has made an acceptable reduction of pore pressure. The total pore pressure obtained for the selected model was equal to 68.6 kPa, while for the main breakwater, by a decrease of 7.8%, this factor was equal to 74.4 kPa. The materials used as filter layers in RMB have a shallow thickness compared to ordinary filters, which have reduced earthworks volume.

1. Introduction

Over time and with the progress of technology in marine structures, RMBs can still be considered the most widely used structures for protecting beaches and ports. RMBs safeguard the coastal area against waves, storms, and currents from the sea, including ports, port facilities, and coastal facilities. RMBs are usually built of ores and stone reinforcement, or artificial concrete reinforcement is used for the outer layers of the structure to ensure its ability to withstand the impact of the waves. Thus, ensuring the stability of these structures is critical. Through the breaker, the flow causes high pressure on the internal pores, and the high pressure in the core can cause amour layer failure and lead to geotechnical instability.

* Corresponding author.
E-mail addresses: p.zanganeh@ guilan.ac.ir (P. Zanganeh Ranjbar)

https://doi.org/10.22124/cse.2023.24252.1053

Geosynthetic with the mechanical characteristics similar to different soil-based materials has now been applied in the infrastructure construction [1,2,3]. Geosynthetic fabrics have been widely used in marine structures over the past five decades. These materials can be an excellent alternative in countries with difficulties accessing stone materials, having to pay a significant cost to transport the material, or not having enough time to build a project. The most crucial issue in the RMB is the pore pressure (PWP) due to the wave. Accurate knowledge of the distribution and reduction of PWPs is essential for designing a stable and safe breakwater. So far, no tools have been proposed to accurately determine the PWPs and associated porous flow fields in the breakwater core [4]. Designing an economic breakwater needs knowledge of the PWP caused by waves in terms of slip stability, filter requirements, wave transmission, wave overflow, and increase in internal water level [5]. Awareness of PWP and wave attenuation inside a porous structure is of great significance as more PWP affects reactions like wave shoaling, wave overflow, reflection, transmission, and hydraulic and geotechnical stability of the breakwater. Reference pressures account for the energy dissipation through the filter and armor layers [4]. The PWP caused by the wave affects RMB behavior in several ways. Accurate knowledge of the distribution and reduction of PWPs is crucial for designing a stable and safe breakwater. There is a constant relationship between the height of the wave that hit and the height of the reference PWP at the point where the filter layer meets the core breaker [5].

The PWP by the wave increases because of the wave period and the water depth. Comparing all the graphs presented for coarse and fine sand shows that the PWP caused by the wave affects the soil parameters more in coarse sand than fine sand [6]. The PWP by the wave decreases exponentially towards the inside of RMB [7]. One can conclude that the increase in pore pressure due to rising water level leads to a decrease in friction resistance in grain soils and swelling in cohesive soils. Changes in water level due to the effect of waves lead to a rapid shift in PWP [8]. Porous water pressure reduces the friction angle between the particles, thus reducing slope stability. When dynamic shock wave loads affect a structure, repetitive loading can cause the development of pore pressure in the ground, which can lead to the lubrication of granular materials [9]. As the breakwater slope increases, the PWP caused by the wave tends to increase in the total depth of the soil. The wave pressure on the seabed surface and the PWP in the seabed in front of the breakwater are high [10]. The lowest amplitude of PWP happens below the breakwater. In all cases, the increase in PWP increases with an increase in wave height in front of the breakwater. Moreover, the wave pressure applied to the breakwater is not imposed directly on the seabed, and the surrounding wave pressure mainly affects the change in PWP below the breakwater. Given the results obtained, the ratio of pore-pressure amplitude decrease with an increase in depth is significant. The PWP decrease in the shallow layer is more effective than the deeper layer [11]. As the amplitude and height of the wave increase, the PWP by the wave increases too. The maximum amplitude of the PWP caused by the wave in each soil condition rises with an increase in the wave period, and with decreasing wave height, the maximum amplitude of the pore caused by the wave decreases in each soil condition [12]. geotextiles are a branch of technical fabrics, fabrics, or permeable fabrics used for various types of civil engineering and other geotechnical applications. The applied areas of geotextiles are extensive, and they have spread very fast worldwide during the last decade. With the rapid progress in technology, geotextiles have found their way into many areas. They are praised worldwide for internal advantages like ease and flexibility in use and softness (compared to monolithic and stone structures). Geotextiles provide a relatively safe and cost-effective solution for day-to-day engineering and construction challenges. As a substitute for natural materials, geotextile products perform various functions like erosion control, soil stabilization, treatment, drainage, separation, and the required reinforcement [13]. Coastal engineering was the starting point for synthetic fabrics in geotechnics in the 1950s. Given the advantages of these fabrics (lightweight, high strength, and long-term strength), the use of woven and non-woven fabrics has recently increased in marine engineering and, more recently, in marine and river engineering, dam construction, railway construction, and tunnels and all fields of geotechnical engineering [14]. In less than 30 years, geosynthetics have brought about a revolution and replaced building materials in some applications. In many cases, using geosynthetics can bring about increased safety, improved performance, and reduced cost compared to traditional design and construction solutions. Geosynthetic uses are usually defined by their basic function. Various geosynthetics exist, like geotextiles, geogrids, geomembranes, and geonets. Geotextiles replace fine-grained filters in drainage cavities to prevent particles from escaping. Moreover, they are used as filters under stonework or armor materials on beaches and in coastal and river protection systems. As drainage, geotextiles allow water to pass through the soil with less permeability [15].

1.2. Anzali free zone' Breakwater

Anzali Free Trade-Industrial Zone is one of the seven free zones of Iran in Guilan. This area is located in the water, soil and coastal zone of Anzali in northern Iran, south of the Caspian Sea and in the north-south corridor. Caspian port complex has two breakwaters, with the length of the east breakwater being 2665 meters and the length of the western one 2435 meters. ***Figure 1*** shows the range of the breakwater examined.

Figure 1. Location of Caspiatn breakwater in Anzali free zone [16].

The height of the western section of this breakwater from the floor to the crown of the breakwater as shown in ***Figure 2*** is 16.32 meters, width 75.51 meters, water height is 11 meters, wave height 5 meters and the dominant wind speed in Anzali is equal to 30 meters per second, and its distance from the beach is 1055 meters. The breakwater examined has several layers of different materials on both the east and west sides, which are based on the MATRESS layer, the core and then covered by the filter and armor layer.

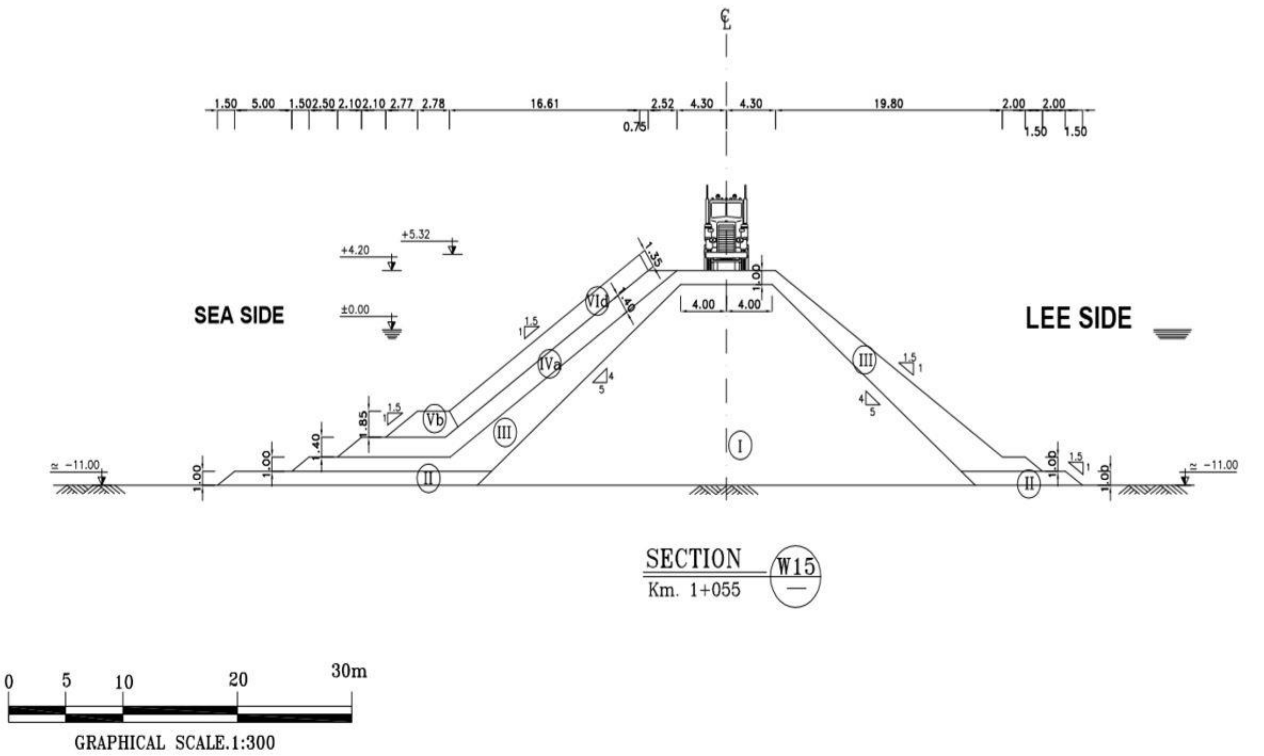

Figure 2. Section W15 West breakwater of Caspian port complex [16].

The economic design of a breakwater calls for knowledge of the PWP caused by the wave in RMB stability, filter requirements, wave transmission, wave overflow, and increase in internal water level. Design features that might be affected by PWP and pore flow as is shown in ***Figure 3***:

A: Slip stability may be severely affected by high pressure in RMB mass and low pressure during the wave backflow on the slope.

B: The state of the wave inside each port basin depends in part on the transmission of the wave through RMB, which mainly depends on the absorption of wave energy because of the flow of porous water.

C: Wave overflow affects the wave state in the port. This is mostly because of the discharge of water seepage into the hill as it progresses, the discharge being an essential feature of the pore flow.

D: The aquifer at the back of the sand-embankment increases by 1 to 2 meters because of the increase in water level by the wave and depending on the flow of characteristics inside the hill [7].

Using geosynthetic materials in geological engineering leaves positive and negative environmental effects. Among the positive effects of these products are their lightness and ease of transportation. Using geosynthetic materials diminishes greenhouse gas emissions significantly. Environmental concerns are because of their plastic state and accumulation after the destruction of the structure. By selecting the appropriate polymer raw materials for using geosynthetic products, one can solve the existing problems [17]. Given the population growth, natural resources are being used extensively as a substitute for synthetic materials, generally derived from fossil fuels (petrochemicals) or minerals, and are operationalized significantly. Thus, natural fibers for technical applications have attracted more attention. A significant political move towards sustainable technologies has been considered to increase awareness of natural materials as a potential source for industrial products. Natural fiber geotextiles have significant environmental benefits in the current global scenario, as they are biodegradable in terms of environmental compatibility. Hence, no synthetic polymers remain in the soil after long service life. The United Nations has declared 2009 the World Year of Natural Fibers to raise global awareness of the importance of natural fibers for producers and industry and consumers and the environment. The development of a sustainable global economy calls for a fundamental change in its approach, improving purchasing power and living standards without wasting resources for future generations. Geotextile materials made from natural fibers 81 based on their photosynthetic CO2 constant should be preferred for environmental reasons. These sustainable resources can be restored in the near future without negative adverse effects on global biodiversity [18].

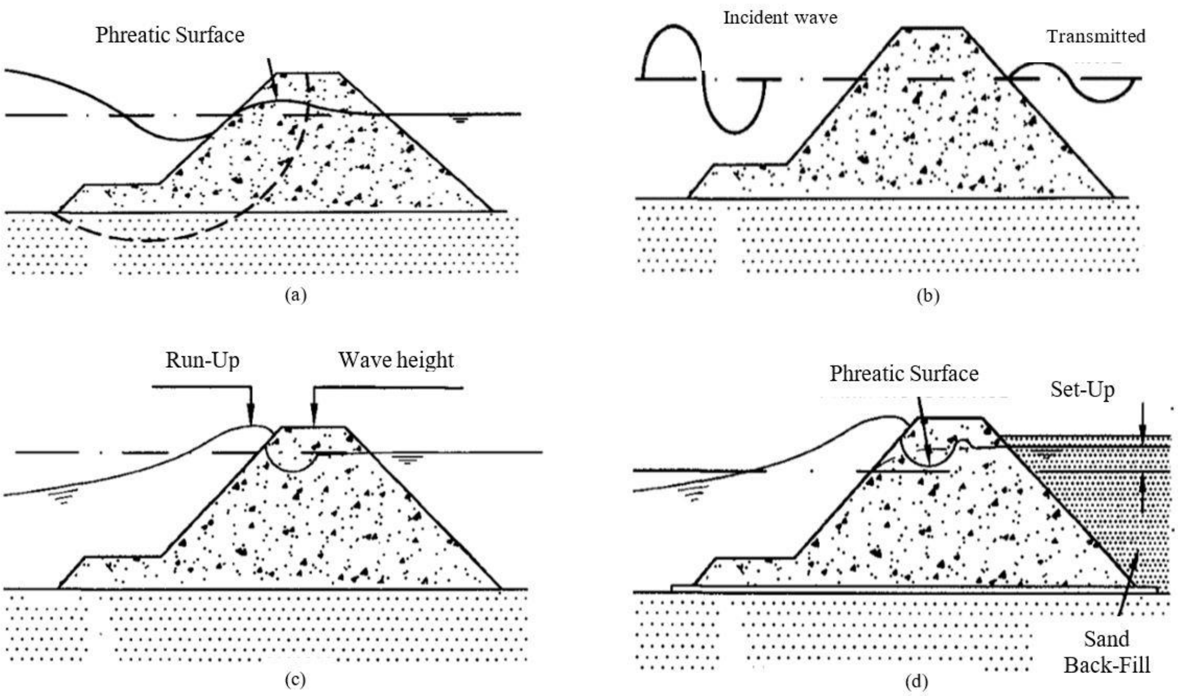

Figure 3. Different types of design under the influence of pore pressure [7].

1.2. Geosynthetic Materials

Geosynthetics is a flat product made of polymeric materials with soil, rock, earth or other materials related to geotechnical engineering as an integral part of human projects, structures, or systems. In 1977, the first geosynthetics Conference in Paris described geosynthetics as an exciting engineering material in civil engineering programs. For instance, they introduced transportation, geotechnics, environment, and hydraulics as private development.

The term geosynthetic is a combination of the two terms “geo” meaning the earth, and as these materials are human-made, the second part “synthetic” means artificial. The materials used in geosynthetics are completely from the plastics industry: they are the polymers made of hydrocarbon, although fiberglass, rubber, and natural materials have been used in their manufacture incidentally [19].

Geotextiles have extensively been used in geotechnical engineering in recent decades, and the global market demand is growing. Geotextiles are mostly made of polyolefin, polyester, or polyamide polymers and polymer series. Geotextiles can be used for geotechnical engineering performances like separation, filtration, strengthening, and erosion control should be used [20]. Geotextiles are particularly suitable for stabilizing and protecting soil surfaces against erosion. Geotextiles are used as erosion control materials to protect the soil from surface water transfer. The purpose of erosion control is to reduce the destructive force of the flow in the ground by absorbing or storing the maximum water and slowing down the movement of soil particles [18].

Geodrains are rolls 1.90m or 3.80m wide and usually 35m or 70m long, quick and easy to install. The prefabricated geodrain overlap configuration provides a fast and straightforward butt-joint connection of geocomposite panels in the longitudinal direction. Using geodrain in earthworks needs less on-site excavation of the material, and if used as a landfill, the containment volume will increase. Using geodrain saves time and natural resources, as 10,000 square meters of geodrain can replace the extraction, transfer, and installation of approximately 3,000 square meters of fine drainage materials [21].

In this study, with the aim of reducing the use of stone materials in order to protect the environment, the use of geosynthetic materials as an alternative to stone layers was investigated. For this purpose, by using the mechanical characteristics of geodrain and geotextile, and replacing them instead of different breakwater layers, modeling was done in order to reduce the pore pressure and its results were analyzed.

2. Methodology

2.1. Modeling in software

GeoStudio is software based on the finite element method (FEM) used to simulate the analysis of geotechnical problems, movement, and distribution of porous water pressure inside porous materials like soil and can simulate two-dimensional problems with axial symmetry. In this software, Seep / w module is used to analyze the mentioned breakwater, which simulates the water flow in the soil and analyzes it.

FEM has become a powerful tool for numerically solving a wide range of engineering problems. The scopes of uses are from deformation and stress analysis of vehicles, aircraft, buildings, and bridge structures to field analysis of heat flow, fluid flow, magnetic flow, water infiltration, and other flow problems. Complex problems can be easily modeled with advances in computer technology. In this analysis method, a complex region is made discrete by defining a chain into simple geometric shapes called finite elements [22].

2.2. Primary breakwater modeling

The modeling should be done so that it well simulates the original model. In the numerical analysis of software using the specifications available in the breakwater, which includes the general geomat of the structure, water height, and components (layers), we started modeling. One of the significant parameters used in the analysis is the hydraulic conductivity or permeability, which according to the specifications given in the breakwater map, can be seen in ***Table 1***. Moreover, the specifications of the materials used in the main breakwater according to ***Figure 2*** are seen in ***Table 2***.

Table 1. The size of the grains used in the breakwater [16].

Type	Weight (KG)	Specification	Area
I	W = 0.1 - 100	50 % > = 50 Kg	365.56 m^2
II	W = 10 - 50	50 % > = 30 Kg	31.79 m^2
III	W = 100 – 600	50 % > = 400 Kg	115.60 m^2
IVa	W = 600 – 1000	50 % > = 800 Kg	43.55 m^2
Vb	W = 1000 – 3000	50 % > = 2000 Kg	8.27 m^2
VId	W = 5600	Antifer	26.94 m^2

Table 2. Introduction of materials used in breakwater [23].

Layer	Material	Permeability
I: Core	Coarse-Grained sand	0.003 m/s
II: Matress	Sand with uniform granulation	0.003 m/s
III: Filter	Rubble	0.004 m/s
IVa: Primary armor	Concrete	0.05 m/s
Vb: Secondary armor	Concrete	0.05 m/s
Vid: Tertiary	Concrete	0.05 m/s

2.3. Alternative materials

In this study, two types of geosynthetics, geodrain and geotextile were used as geocomposite materials. The geotextile material used as the filter layer is GMH 250, with a thickness of 0.0021 m/s and permeability of 0.0024 m/s. The geodrain materials used in the model instead of the stone filter layer called (APT-T7) with the specifications: the thickness of 0.003 meters and permeability of 0.00015 m/s. The characteristics of the alternative materials are given in ***Tables 3*** and ***4***, respectively, for geotextile and geodrain materials.

Table 3. Specification of geotextile materials [23].

Properties	Test Method (ASTM)	Unit	GMH 200	GMH 250	GMH 300	GMH 400	GMH 500	GMH 600	GMH 700	GMH 800	GMH 900	GMH 1000
PHYSICAL PROPERTIES												
Mass	D-5261	gr/m^2	200	250	300	400	500	600	700	800	900	1000
Thickness	D-5199	mm	1.50	2.10	2.80	3.40	4.20	4.80	5.20	5.80	6.50	8.00
MECHANICAL PROPERTIES												
Grab Tensile Strength	D-4632	N	600	700	820	1200	1450	1800	2000	2480	3000	3400
Grab Elongation	D-4632	%	>50	>50	>50	>50	>50	>50	>50	>50	>50	>50
Mullen Burst	D-3786	kPa	2200	2450	3300	4400	5300	6300	7000	7800	8300	9000
Trapezoidal Tear Strength	D-4533	N	450	365	650	900	1050	800	1010	1110	1250	1390
Puncture Strength	D-4833	N	400	510	720	930	1150	1300	1450	1600	1780	2000

Wide Width Tensile	D-4559	KN/m	8	10	12	16	22	26	30	36	40	50
CBR Puncture	D-6241	N	800	1400	2000	2300	2700	3100	3600	4350	4850	5400
UV Resistance @500 hr	D-4355	%	>90	>90	>90	>90	>90	>90	>90	>90	>90	>90
HYDRAULIC PROPERTIES												
Apparent Opening Size (A.O.S)	D-4751	mm	.024	0.21	0.20	0.15	0.15	0.11	0.09	0.09	0.07	0.06
Permittivity	D-4491	Sec^{-1}	2.40	2.20	1.90	1.60	1.30	1.20	1.00	0.95	0.90	0.75
Permeability	D-4491	Cm/sec	0.22	0.24	0.23	0.24	0.24	0.28	0.28	0.21	0.21	0.21
Flow Rate	D-4491	L/m^2 /sec	120	110	100	95	85	80	75	60	50	45

Table 4. Specification of geodrain materials [24]

TYPICAL PROPERTIES		**STANDARD**	**UNIT**	**APT – T7**	**APT – T7 A**	**APT – T9**
CORE	Configuration			----------------	----------------	----------------
	Raw material			PP/PE/PET	PP/PE/PET	PP/PE/PET
Weight	Drain	ASTM D 1777	g/m	65 ± 5	65 ± 5	70 ± 5
Width		ASTM D 3774	mm	100 ± 5	100 ± 5	100 ± 5
Thicknes s	(Core+Filter)	ASTM D 5199	mm	3.0 ± 0.2	3.2 ± 0.2	4.2 ± 0.2
DRAIN						
Tensile strength		ASTM D 4596	kN	≥ 1.7	≥ 1.7	≥ 2.0
Grab tensile strength		ASTM D 4632	kN	≥ 1.6	≥ 1.6	≥ 1.7
Elongation at break		ASTM D 4595	%	≥ 20	≥ 20	≥ 20
Elongation at 0.5Kn		ASTM D 4632	%	< 10	< 10	< 10
Discharge capacity press 10kPa, i =0.5		ASTM D 4716	$\times 10^{-8}$ m^2/s	≥ 80	≥ 80	≥ 80
Discharge capacity press 350kPa, i =0.5		ASTM D 4716	$\times 10^{-8}$ m^2/s	> 60	> 60	> 60
Discharge capacity press 400kPa, i =0.5		ASTM D 4716	$\times 10^{-8}$ m^2/s	> 60	> 60	> 60
FILTER						
Tensile strength		ASTM D 4595	kN/m	≥ 4	≥ 4	≥ 7
Grab strength		ASTM D 4632	N	≥ 300	≥ 300	≥ 500
Permeability		ASTM D 4491	$\times 10^{-4}$ m/s	≥ 1.5	≥ 1.5	≥ 1.5
Apparent Opening Size (AOS) based on O_{95}		ASTM D 4751	µm	< 75	< 75	< 75
Burst Strength		ASTM D 3786	kPa		> 900	> 900
Tear Strength		ASTM D 4533	N		> 100	> 100
Puncture Resistance			N		> 100	> 100
TRANSPORTATION DETAILS						
Length Roll			m	300	300	225
Outside Diameter			m	1.15	1.15	1.35
Roll Weight			kg	20	20	23
Container 40ft			m	150.000	150.000	110.000
Unite price (EXW)			USD/m	0.102	0.125	0.152

3. Results and Discussion

3.1. Primary breakwater modeling

Figure 4 shows a prototype of the Caspian breakwater run in the software. The height of the wave colliding with the breakwater for all the models made is 5 meters, and the water height on both sides of the breakwater - the lee side and the seaside - is 11 meters. Another important parameter is to determine the boundary conditions of the target in the structure, which for the upstream conditions is (seaside) is 13.5 m height and for the downstream (lee side) 11 m height.

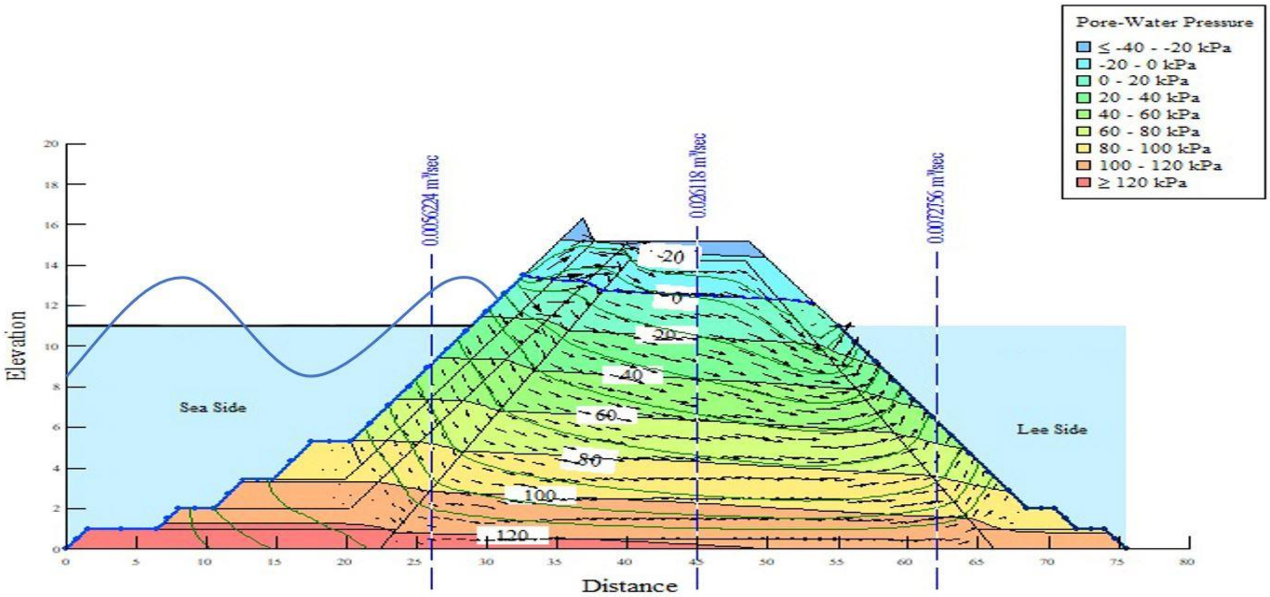

Figure 4. Primary breakwater numerical model

A table is seen in the right-hand corner that shows the PWP from the lowest value - the upper part of the structure (crown) - to the lowest part of the structure in the breakwater floor in terms of kilopascals in the model. A phreatic line is visible in the figure that shows the PWP. This pressure for the top and bottom of the phreatic line has shown remarkable figures. The phreatic line or static line marks the boundary between the dry and wet areas in the breakwater. The upper areas of this line in the breakwater show negative pore pressure, and the lower areas the positive pore pressure. In numerical modeling for the initial breakwater, the PWP range for the highest breakwater point above the phreatic line (crown) is -30.8522 and at the lowest breakwater point below the phreatic line at the floor is about 125.5338 kPa. As ***Figure 4*** shows, there are three flow sections on the sea, center, and lee sides, which are 0.0056254, 0.026118, and 0.0072756 m3/s, respectively. In this model, PWP is randomly investigated at the nearest points of the existing elements of the water surface (11 meters), whose results are shown in ***Table 5***.

Table 5. Investigation of pore pressure in the primary model of breakwater

X(m)	36	39	43	45	53
PWP (kPa)	17.0999	19.4135	15.0391	15.6315	9.2600

As is seen in the curve in ***Figure 5***, PWP at a distance of 36 meters from the sea (Seaside) starts from 17.0999 kPa and the PWP at a distance of 39 m is facing a relative increase that reaches

19.4135 kPa. Nevertheless, gradually with the advance towards the lee side, the PWP is reduced so that at the end of the breakwater - a distance of 53 meters - we witness a decrease of 1.7 times compared to 39 meters, which is 9.26 kPa. The vertical axis of this diagram shows PWP, and the horizontal one shows the distance of the points.

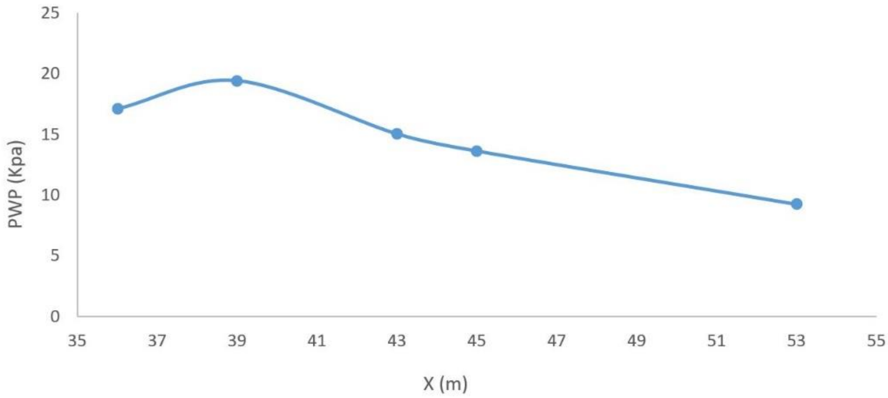

Figure 5. The pore pressure curve in in the primary breakwater

3.2 Modeling using geotextiles and geodrain in filters

Figures 6 and ***7*** show two types of modeling where the breakwater filter materials are completely removed and the filter materials are replaced in two stages. In the first stage of modeling, geotextile materials have been applied as the first layer and geodrain as the second, and in the second stage of modeling, geodrain was applied as the first layer of the filter and geotextile as the second, respectively.

As ***Figure 6*** shows, in this modeling, after replacing the geotextile and geodrain instead of the rock filter layer, we achieved the results ahead. The purpose of this modeling was to achieve a low PWP. PWP range in this numerical model was obtained at the highest breakwater point as -32.7778 and at the lowest breakwater point 126.5450 kPa. The cross-section of the current on the seaside, the center of the breakwater, and the lee side are 0.0092243, 0.061949, and 0.02427 m3/s, respectively. PWP is done according to the previous model, as is seen in ***Table 6***.

In the study done in this numerical model, the value of PWP at a distance of 36 meters from the seaside had the highest PWP of 23.5771 kPa close to the water level (11 meters). However, at a distance of 45 meters, we see an increase in PWP again. Finally, at a distance of 53 meters near the shore, this value decreases significantly, which was 1.9 times compared to the distance of 45 meters, showing 5.0164 kPa.

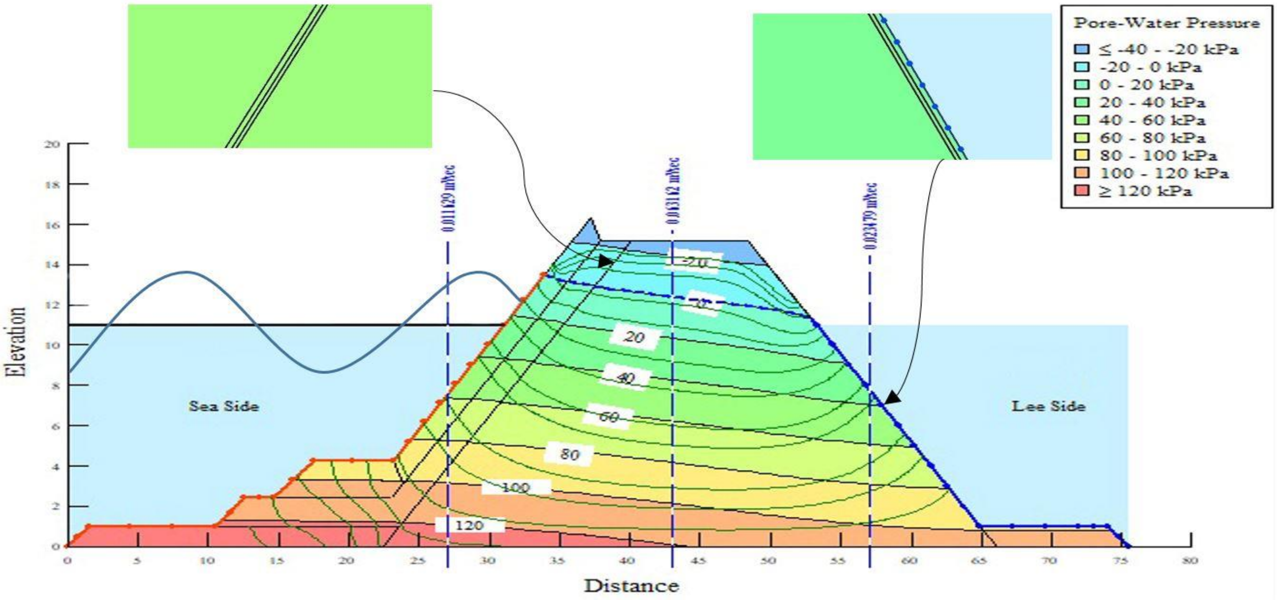

Figure 6. Use of geotextile and geodrain as filter layer

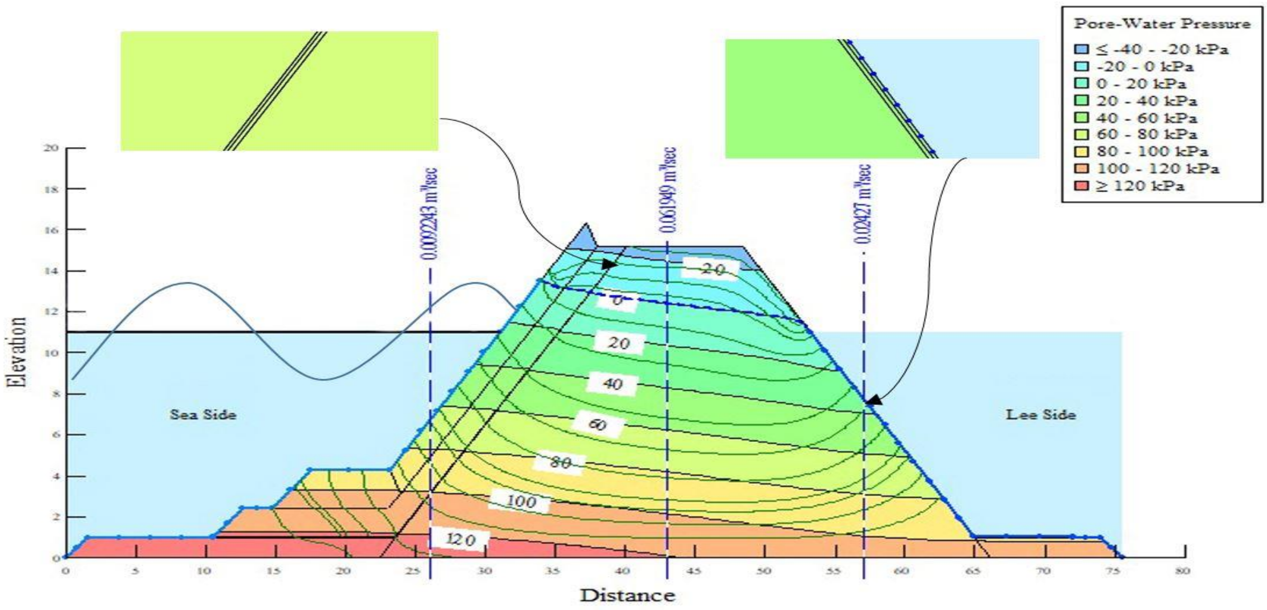

Figure 7. Use of geodrain and geotextile as filter layer

Table 6. The amount of pore pressure when using geotextile and geodrain

X(m)	36	39	43	45	53
PWP (kPa)	23.5771	16.7176	16.5412	17.3196	5.0164

Figure 8 shows the curve of this analysis. Modeling done using geodrain and geotextile in the filter is obtained as the first and second layers. The following results are the values obtained from this numerical modeling, as PWP at the highest point of the breakwater is -32.790901 and at the lowest point 125.12764 kPa. The flow rate at three points in the breakwater areas is from the seaside, the center of the breakwater, and the lee side are 0.011629, 0.063162, and 0.023479 m3/s. ***Table 7*** shows the PWP obtained from this modeling.

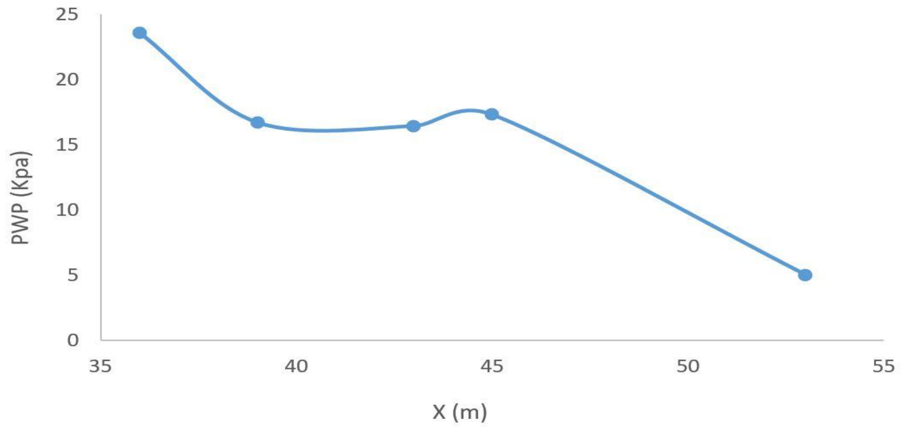

Figure 8. The pore pressure curve when using geotextile and geodrain

Table 7. The amount of pore pressure when using geodrain and geotextile

X(m)	36	39	43	45	53
PWP (kPa)	23.5096	16.3283	14.2287	11.4827	3.0556

In this numerical model, the maximum PWP is 36 meters at 23.5096 kPa. As we get closer to the lee side, this value decreases gradually, with the minimum value 3.0556, occurring at a distance of 53 meters, and the figure is remarkable. ***Figure 9*** shows the curve obtained from the analysis of these results.

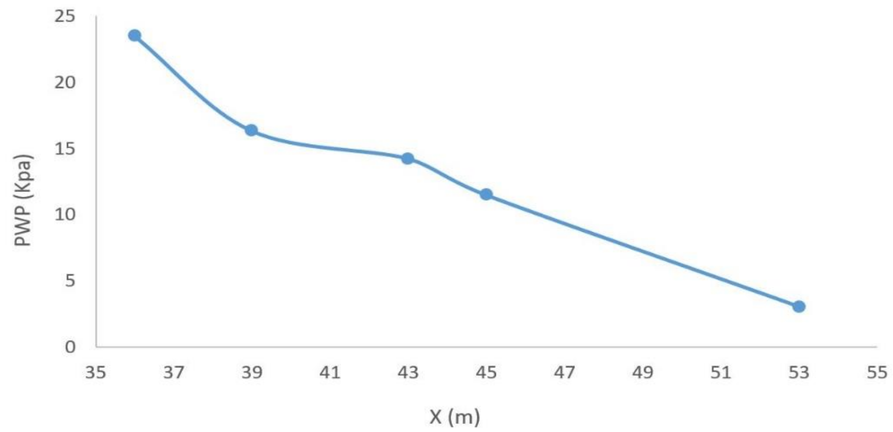

Figure 9. The pore pressure curve when using Geodrain and Geotextile

3.3 Modeling in case of using geocomposite as a secondary armor layer and filter

According to the modeling done in the previous cases, besides the filter layer, we removed the secondary armor layer of reinforcement and used geocomposite instead, so that geodrain was the first layer and geotextile was the second layer and vice versa. We will use this modeling. In ***Figure 10***, besides removing the filter layer, we replaced the secondary layer of armor with geodrain and geotextile in this modeling. The data obtained from this modeling are PWP at the highest level of the structure was -32.782908 and at the floor of the structure 125.14992 kPa. The cross-section flow or water discharge at the seaside, the center of the structure, and the lee side are 0.011788, 0.063223, and 0.023502 m3/s.

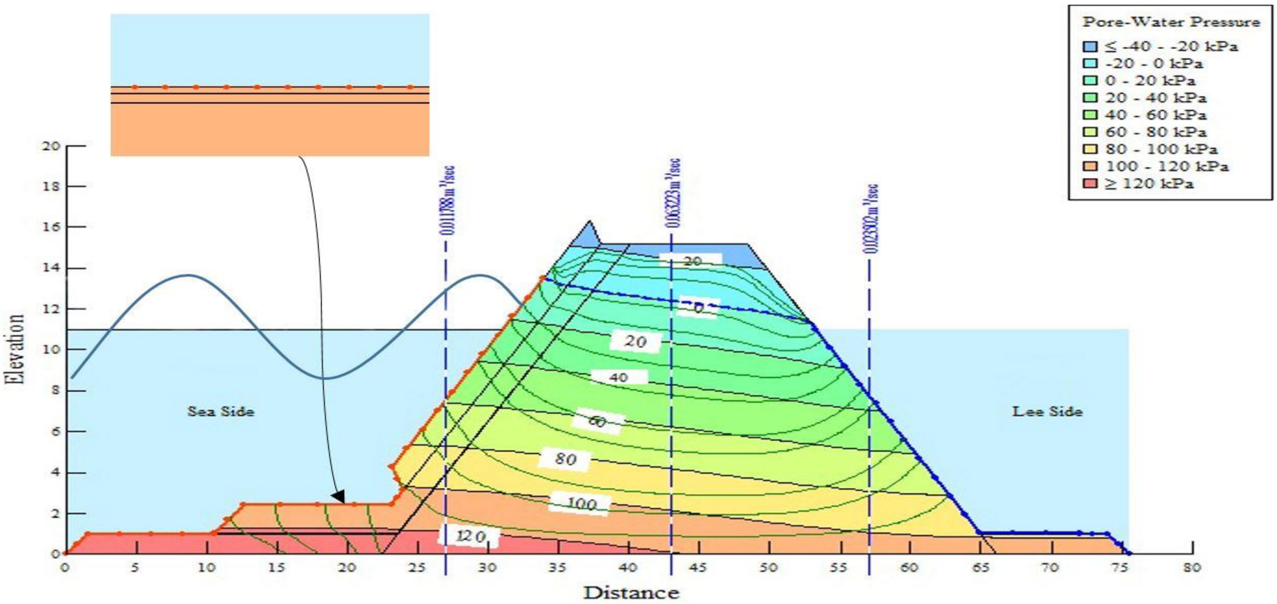

Figure 10. Use of geodrain and geotextile as filter layer and secondary armor layer

The PWP obtained from this numerical model at 5 random points in RMB can be seen in ***Table 8***.

Table 8. The amount of pore pressure when using geodrain and geotextile as secondary armor and filter layer

X(m)	36	39	43	45	53
PWP (kPa)	23.5218	16.3732	14.2861	11.5591	5.0507

PWP started at 36 meters from 23.5218 kPa and has the highest value. Like the previous modeling, PWP value gradually decreased as we moved towards the shore. In this model, the lowest PWP - 5.0507 kPa - was 52 meters from the breakwater near the shore. ***Figure 11*** shows the results curve obtained from this modeling.

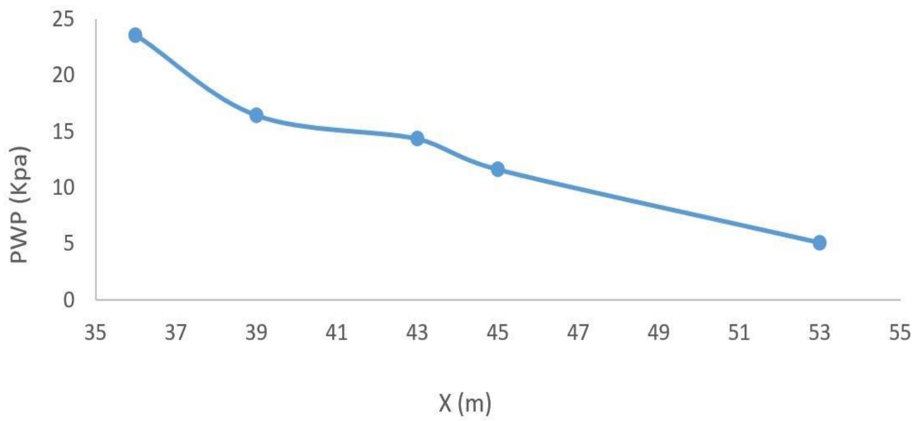

Figure 11. The pore pressure curve when using geodrain and geotextile as secondary armor and filter layer

In ***Figure 12***, this modeling has used geotextile as the first layer in the filter and the armor and geodrain as the second layer. The following results are the values obtained from the PWP breakwater is -32.794824 kPa and at the lowest point 125.25551 kPa. The three crossing points of the flow created on the seaside, at the center of the breakwater and on the lee side show the values of 0.0138988, 0.062261 and 0.0058741 m3/s, respectively.

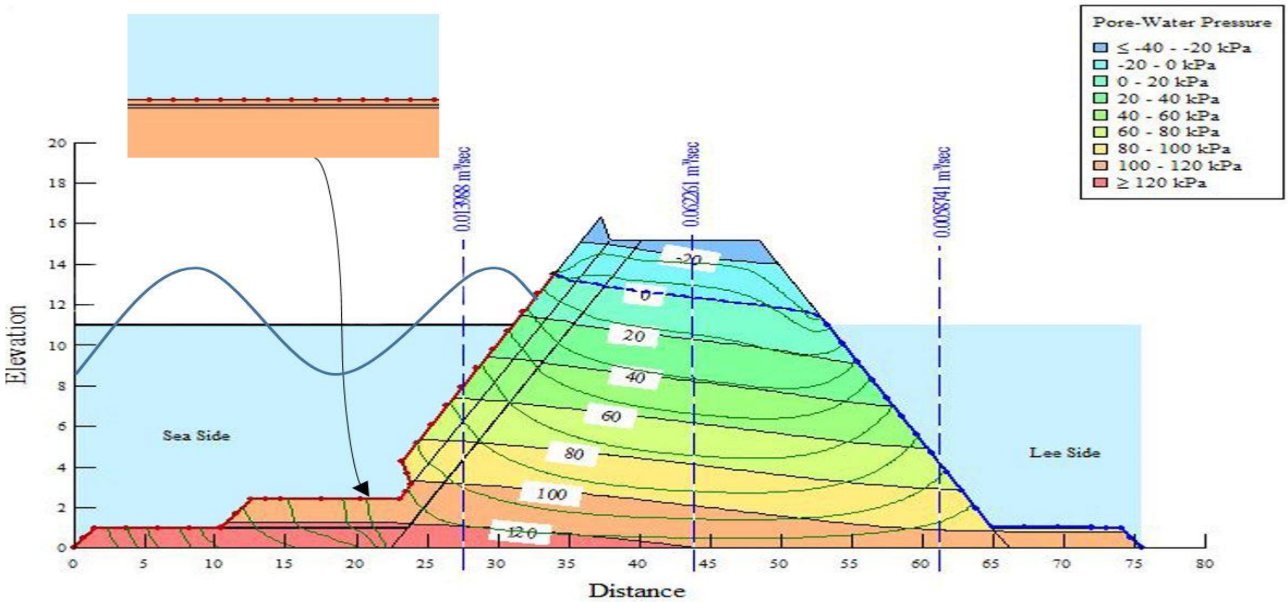

Figure 12. Use of geotextile and geodrain as filter layer and secondary armor layer

The PWP values obtained from this model are given in ***Table 9***.

Table 9. The amount of pore pressure when using geotextile and geodrain as secondary armor and filter layer

X(m)	36	39	43	45	53
PWP (kPa)	23.6084	16.5697	12.5221	12.9398	5.0585

According to the results obtained from this modeling, the PWP at a distance of 36 meters from the sea shows the value of 23.6084 kPa, which is the highest value in this model. However, this value gradually decreases, and at the endpoint considered near the sea - a distance of 53 meters - this value shows 5.0585, which is very acceptable compared to the main breakwater. Then ***Figure 13*** shows the relevant curves to this modeling.

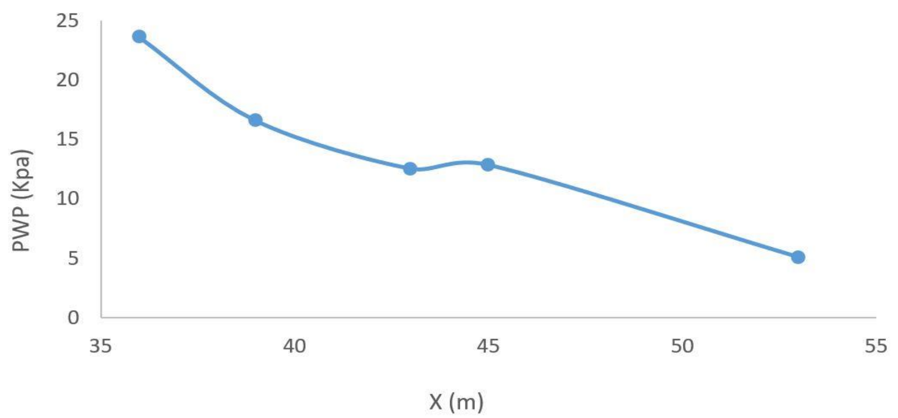

Figure 13. The pore pressure curve when using geotextile and geodrain as secondary armor and filter layer

3.4 Using geomat as the MATRESS layer and geocomposite as a filter layer in the breakwater

The geomat used in the study has a permeability of 0.00003 m/s and a thickness of 0.00052 meters. Other properties of these materials are given in ***Table 10*** [25].

Table 10. Specification of geomat materials [25].

Geotextile usage	Thickness (mm)	Mass per m^2 (g/m^2)	AOS O_{95} (mm)	Permeability (m/s)	Tensile strenght (kN/m)		Max. elongation (%)	
					Longitudinal	Transverse	Longitudinal	Transverse
Mat	0.52	131	0.145	3×10^{-5}	28	26	20.5	17.5
Base layer	0.53	152	0.152	3×10^{-5}	33	77	22.0	16.0
Geotextile matress	0.61	284	0.088	4×10^{-5}	60	55	25.0	22.0

In this modeling, various states, geodrain, and geotextile will be the filter layer, and geomat will be used as an alternative in the breakwater. It has to be noted that the material of the MATRESS materials is sand with uniform granulation. Refer to ***Table 2*** for more information. ***Figure 14*** shows the geodrain as the first layer, the geotextile of the second layer as a filter, and the geomat as MATRESS. In modeling, geodrain and geotextile have been introduced as the first and second layers of the filter and geomat as the MATRESS layer. PWPs obtained at the highest and th e lowest points are -32.866817 and 125.14782 kPa. The flow rates in three sections on the seaside, in the center of the breakwater and on the lee side are 0.010182, 0.063244 and 0.016542, respectively.

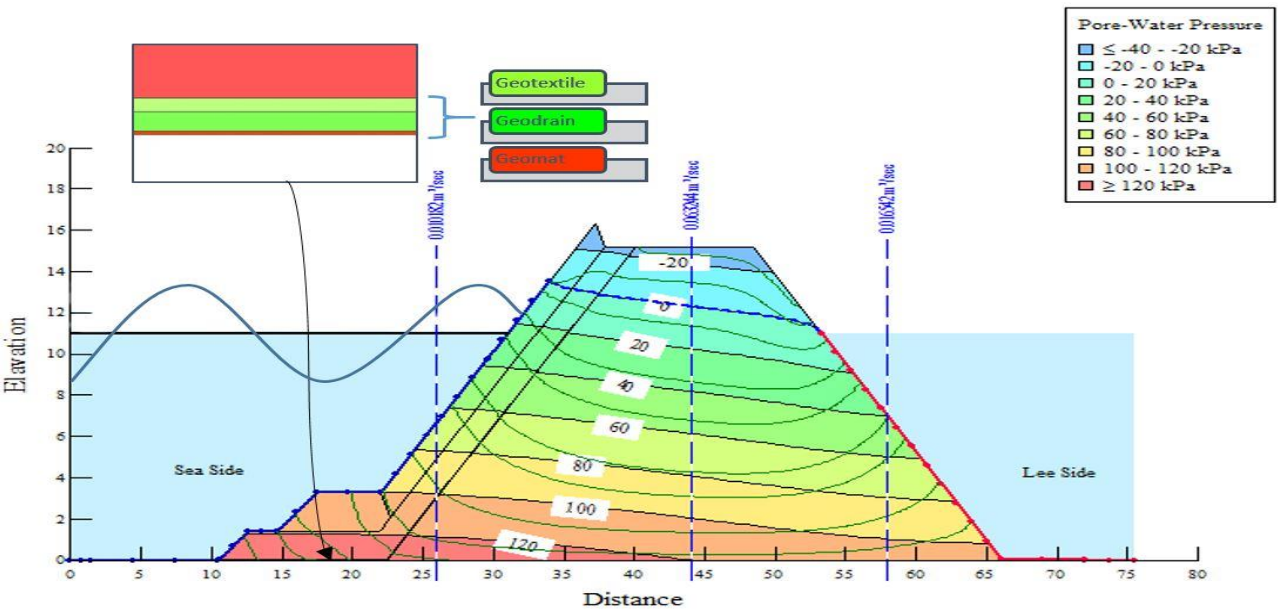

Figure 14. Use of geodrain and geotextile as filter layer and geomat as matress

Table 11 shows the PWP values obtained from this modeling.

Table 11. The amount of pore pressure when using geodrain and geotextile as filter layer and geomat as matress

X(m)	36	39	43	45	53
PWP (kPa)	24.6588	17.2956	13.2997	12.3012	4.1542

Based on the results, PWP value at a distance of 36 meters is 24.6588 kPa, which is the highest value, the PWP value reduce by moving in the structure and at a distance of 53 meters from the sea reaches the lowest possible value of 4.1542 kPa. The resulting curve is shown in ***Figure 15***.

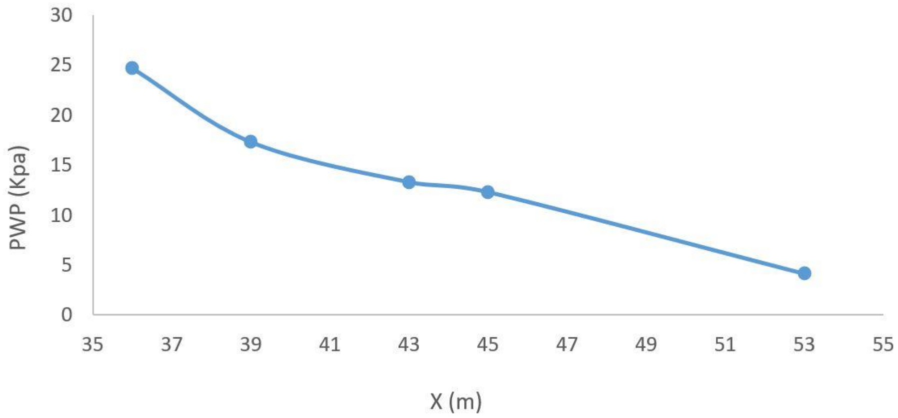

Figure 15. The pore pressure curve when using geodrain and geotextile as filter layer and geomat as matress

In the modeling ahead, we have changed the place of geodrain and geotextile in the filter layer and geomat has been used as a constant in the MATRESS. According to the modeling, the value of PWP is -32.803846 at the highest point of the breakwater and for the bottom of the point in the floor of the breakwater 125.30869 kPa. The section discharge in the lee area is 0.0098809, in the middle part of the breakwater 0.062141 and the last section on the seaside 0.017228 m3/s. The model obtained is shown in ***Figure 16***.

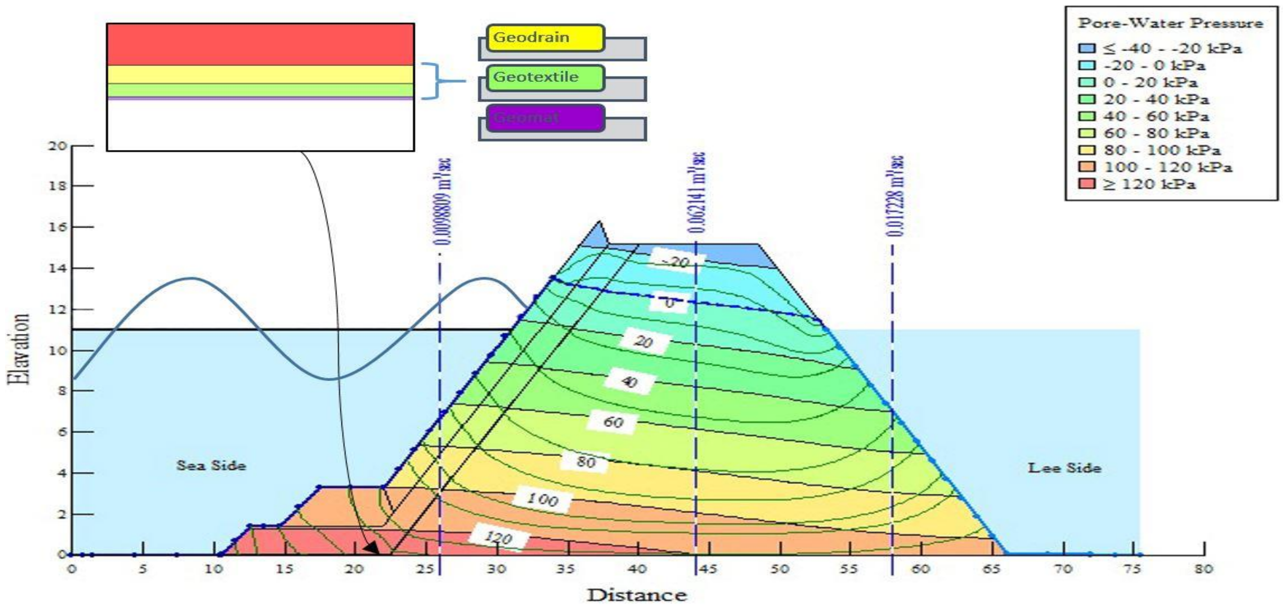

Figure 16. Use of geotextile and geodrain as filter layer and geomat as matress

PWP obtained at the random points of this modeling is given in ***Table 12***.

Table 12. The amount of pore pressure when using geotextile and geodrain as filter layer and geomat as matress

X(m)	36	39	43	45	53
PWP (kPa)	24/8262	17.5250	13.5874	12.6356	6.0318

Figure 17 shows PWP curve for a better understanding of where the PWP is initially at its highest level of 24.8262 kPa, and gradually as we move towards the lee side, this value decreases. The lowest possible value is 6.0318 kPa at 53 meters, and the PWP values were close at distances of 43 and 45 meters.

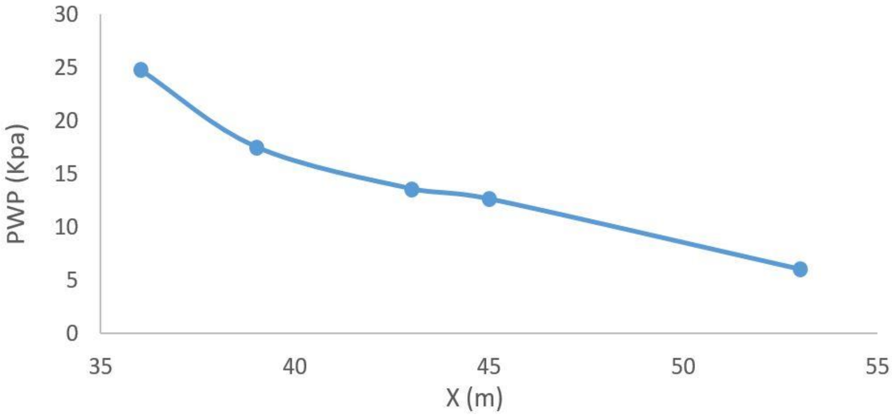

Figure 17. The pore pressure curve when using geotextile and geodrain as filter layer and geomat as matress

3.5 Using geomat as a MATRESS layer and geocomposite as a filter and armor layer in the breakwater

Among the other possible causes in reducing PWP in the breakwater are the simultaneous placement of geosynthetic materials in the filter layer and secondary armor and MATRESS. In the modeling ahead, we will place all the items in order.

Using geodrain and geotextile in the filter layer and secondary armor, geomat as the MATRESS layer and the result obtained from this model are given in ***Figure 18***.

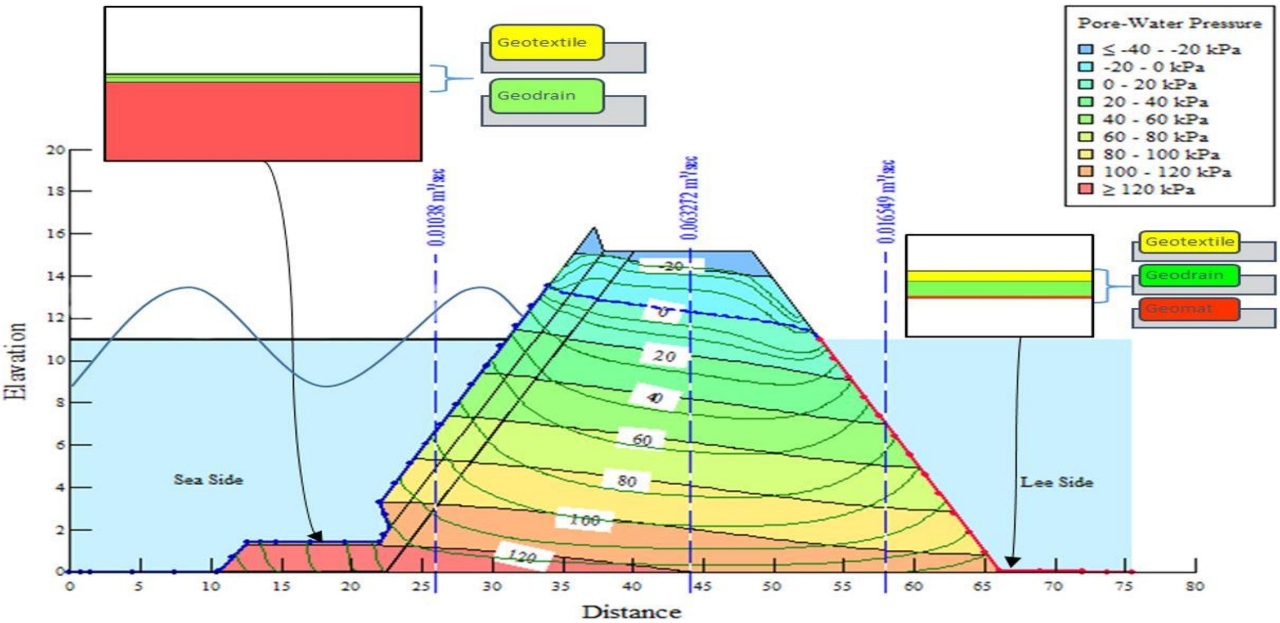

Figure 18. The model obtained from the use of geodrain and geotextile in filter and armor and geomat in matress

In this modeling, geodrain is used as the first layer and geotextile as the second layer in the filter and secondary armor. As already stated, mentioned before, geomat is a layer of MATRESS. The values of PWP at the highest and the lowest point of the breakwater are -32.863257 and 125.15966 kPa, respectively. The flow values on the seaside, the center of the structure, and the lee sides are, respectively, 0.01038, 0.063272, and 0.016549 m3/s.

Table 13 shows the PWP values at random points obtained from this type of modeling.

Table 13. The amount of pore pressure when using geotextile and geodrain as filter, armor and geomat as matress

X(m)	36	39	43	45	53
PWP (kPa)	24.6642	17.301	13.3047	12.3056	5.9646

By studying the results obtained from this modeling, the highest PWP is obtained at a distance of 36 meters from the seaside and a distance of 53 meters, 5.9643 kPa. At distances 43 and 45 meters, PWP breakwater shows a difference of approximately 1 kPa. The PWP curve in this model is shown in ***Figure 19***.

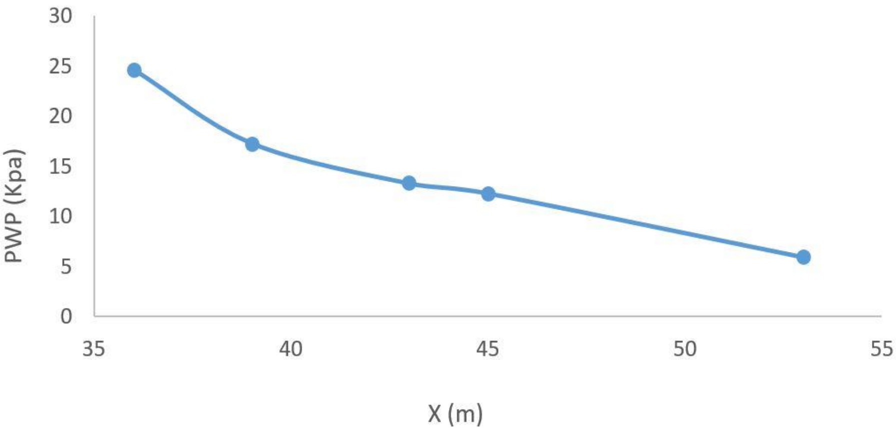

Figure 19. The pore pressure curve when using geotextile and geodrain as filter, armor and geomat as matress

The modeling done in ***Figure 20*** is the same as the previous model, except that the place of geodrain and geotextile materials in the secondary armor and the filter layer has changed and geomat remains constant as a layer of MATRESS. The last model is that geotextile is used as the first layer and geodrain as the second. The value of PWP at the highest point is -31.930749, and at the lowest, 125.57348 kPa. The section of the flow on the seaside is 0.0095913, in the center of the breakwater 0.063786, and on the lee side 0.017662 m3/s.

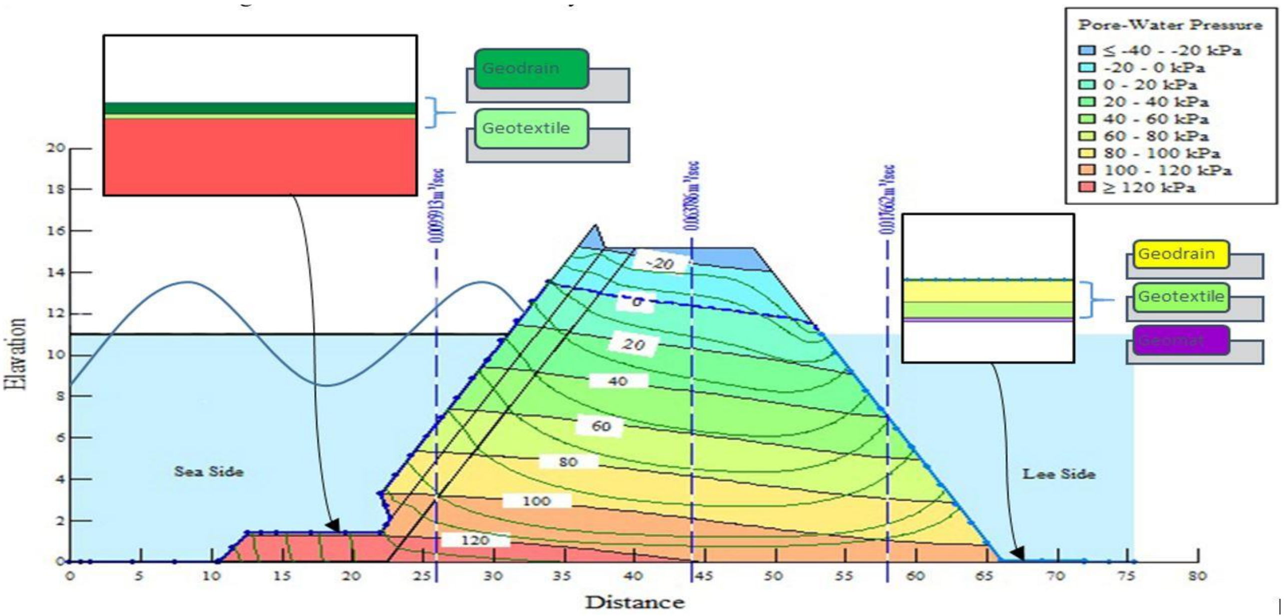

Figure 20. The model obtained from the use of geotextile and geodrain as filter, armor and geomat as matres

Table 14 shows PWP values obtained from random points in this modeling.

Table 14. The amount of pore pressure when using geodrain and geotextile as filter, armor and geomat as matress

X(m)	36	39	43	45	53
PWP (kPa)	25.3065	18.0370	14.0075	12.9893	6.0817

As is seen in the chart obtained from this modeling in ***Figure 21***, maximum PWP value is obtained at a distance of 36 meters, 23.3065 kPa, and as it moves towards the lee side, its value gradually reduces, eventually reaching its lowest value of 6.0817 kPa.

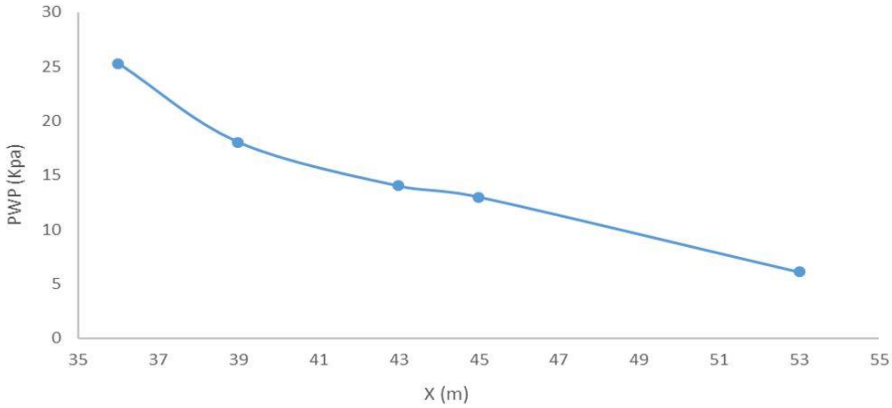

Figure 21. The pore pressure curve when using geodrain and geotextile as filter, armor and geomat as matress

3.6 Comparison of modeling results

This section intends to compare the modeling done and state the best option with the most reduction in PWP. ***Table 15*** shows PWP values of all models. Reviewing this table, one can conclude that all models have acceptable results compared to the main breakwater, but the best option is to use geodrain as the first layer and geotextile as the second layer of the filter.

Table 15. Comparison of pore pressure in all models

X(m)	**36**	**39**	**43**	**45**	**53**
PWP $_{KPa}$ (Main breakwater)	17.0999	19.4135	15.0391	13.6315	9.2600
PWP $_{KPa}$ (Geodrain + Geotextile)=Filter	23.5096	16.3283	14.2287	11.4827	3.0556
PWP $_{KPa}$ =(Geodrain+Geotextile)=Sencond Armor	23.5218	16.3732	14.2861	11.5591	5.0507
PWP $_{KPa}$ =(Geotextile+Geodrain)=Sencond Armor	23.6084	16.5697	12.5221	12.8398	5.0585
PWP $_{KPa}$ (Geotextile + Geodrain)=Filter	23.5771	16.7176	16.4512	17.3196	5.0164
PWP $_{KPa}$ (Geodrain+Geotextile)=Filter Geomat= Matress	24.6588	17.2956	13.2997	12.3012	4.1542
PWP $_{KPa}$ (Geodrain+Geotextile)=Filter + Armor Geomat= Matress	24.6642	17.3010	13.3047	12.3056	5.9643
PWP $_{KPa}$ (Geotextile+Geodrain)=Filter Geomat= Matress	24.8262	17.5250	13.5874	12.6356	6.0318
PWP $_{KPa}$ (Geotextile+Geodrain)=Filter + Armor Geomat= Matress	25.3065	18.0370	14.0075	12.9893	6.0817

Figure 22 shows the PWP curve obtained from these results. While starting calculating at the 36-meter point, the initial breakwater has the lowest PWP, and all the values were close together at

the start in the following nine modeling modes, ranging from about 23 to 25 kPa. Among the other points seen in this curve is the proximity of the geodrain + geotextile model data with the secondary armor model, which has reached a very close PWP up to 45 meters away from the relevant numbers, and the next one is geodrain + geotextiles reaching a more desired value at a distance of 52 meters.

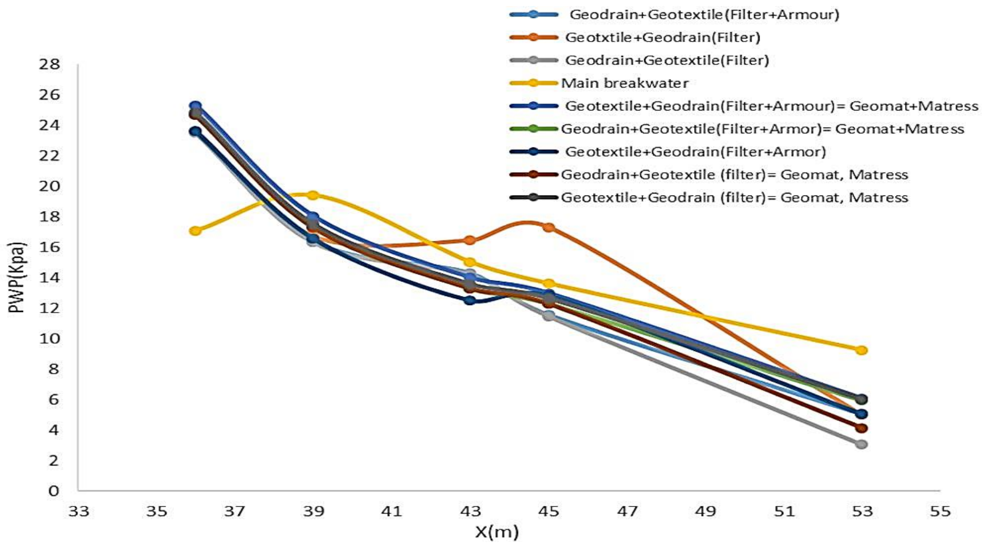

Figure 22. Comparison of pore pressure curve in all models

4. Conclusion

The phenomenon of pore pressure has always been an essential issue in breakwater structures. This article investigated this phenomenon and proposed solutions to reduce pore pressure. Due to technological advances in construction materials, In the past few decades, the Goesynthetic materials have shown an outstanding performance in civil works, and in this research, these materials have been used to reduce pore pressure. Geosynthetic materials that we have used as a part of the main components in RMB are; geotextile, geodrain, and geomat. The result shows that using geosynthetic materials as a filter layer has reduced the pore pressure in the core of RMB. The total pore pressure obtained for the selected model, geodrian was the first and geotextile was the second layer, was equal to 68.6 KPa. For the main breakwater, this factor was equal to 74.4 KPa. We have seen a decrease of 7.8% in pore pressure in the core of RMB. The materials used as filter layers in RMB have a shallow thickness compared to ordinary filters, which have reduced the volume of earthworks at the filter. Geosynthetics have excellent environmental benefits, as they are biodegradable in terms of environmental compatibility, so no synthetic polymers remain in the soil after long service life.

References

[1] Rezvani, R. (2020). "Shearing response of geotextile-reinforced calcareous soils using monotonic triaxial tests." Marine Georesources & Geotechnology 38(2): 238-249.

[2] Rezvani, R., I. Hosseinpour and M. Kavoshmelli (2022). "Effect of moisture content on unconfined compressive behavior of geotextile-reinforced clay specimen." Arabian Journal of Geosciences 15(3): 230.

[3] Hosseinpour, I., R. Rezvani and M. Kavoshmelli (2023). "Experimental investigation of the behavior of cemented-clay specimen reinforced with geotextile layers." Journal of Structural and Construction Engineering: -.

[4] Vanneste, D., & Troch, P. A. (2010). Experimental research on pore pressure attenuation in rubble-mound breakwaters. Paper presented at *the 32nd International Conference on Coastal Engineering*, ICCE 2010.
[5] Troch, P. (2001). Experimental study and numerical modelling of pore pressure attenuation inside a rubble mound breakwater. *PIANC Bulletin* No, 108.
[6] Jeng, D., Cha, D., Lin, Y., & Hu, P. (2001). Wave-induced pore pressure around a composite breakwater. *Ocean Engineering*, 28(10), 1413-1435.
[7] De Groot, M., Yamazaki, H., Van Gent, M., & Kheyruri, Z. (1995). Pore pressures in rubble mound breakwaters. *Coastal Engineering*, pp.1727-1738.
[8] Iranian port and marine structures design regulations. (2006):5-300.
[9] Bruun, P., (2013). Design and construction of mounds for breakwaters and coastal protection. Elsevier.
[10] Liao, C., Tong, D., Jeng, D.-S., & Zhao, H. (2018). Numerical study for wave-induced oscillatorypore pressures and liquefaction around impermeable slope breakwater heads. *Ocean Engineering*, 157, 364-375.
[11] Zhai, Y., Zhang, J., Jiang, L., Xie, Q., & Chen, H. (2018). Experimental study of wave motion and pore pressure around a submerged impermeable breakwater in a sandy seabed. *International Journal of Offshore and Polar Engineering*, 28(01), 87-95.
[12] Liu, B., Jeng, D. S., Ye, G. L., & Yang, B. (2015). Laboratory study for pore pressures in sandy deposit under wave loading. *Ocean Engineering*, 106, 207-219. doi:10.1016/j.oceaneng.2015.06.029
[13] Ashis, M. (2015). Application of geotextiles in coastal protection and coastal engineering works: an overview. *Int. Res. J. Environ. Sci*, 4(4), 96-103.
[14] Heerten, G. (1984). Geotextiles in coastal engineering—25 years experience. *Geotextiles and Geomembranes*, 1(2), 119-141.
[15] Holtz, R. D. (2001). Geosynthetics for soil reinforcement. Seattle, Washington.
[16] Sea port and consulting engineers (2008), " Album of executive plans of east and west breakwaters of Caspian port complex ".
[17] Müller, W.W. and Saathoff, F., (2015). Geosynthetics in geoenvironmental engineering. *Science and technology of advanced materials*, 16(3), p.034605.
[18] Desai, A.N. and Kant, R., (2016). Geotextiles made from natural fibres. In *Geotextiles* (pp. 61-87). Woodhead Publishing.
[19] Koerner, R. M. (2012). Designing with geosynthetics (Vol. 1): Xlibris Corporation.
[20] Wu, H., Yao, C., Li, C., Miao, M., Zhong, Y., Lu, Y. and Liu, T., 2020. Review of application and innovation of geotextiles in geotechnical engineering. *Materials*, 13(7), p.1774.
[21] Naue Gmbh & Co.KG, (2018). Material specification. Koln, Germany.
[22] Chandrupatla, T.R., Belegundu, A.D., Ramesh, T. and Ray, C., (2002). Introduction to finite elements in engineering (Vol. 10). Upper Saddle River, NJ: Prentice Hall.
[23] Ebadi, M. (2018). Investigation the possibility of using geotextiles as a part of the filter layer in rubble mound breakwater. M.Sc. thesis.
[24] Thaichau, APT Geotextile, (2015). Specifications of Drain". Ho Chi Minh City, Viet Nam.
[25] Yan, S.W. and Chu, J., (2010). Construction of an offshore dike using slurry filled geotextile mats. *Geotextiles and Geomembranes*, 28(5), pp.422-433.